Control-oriented modeling of servo-pump driven injection molding machines in the filling and packing phase

authored by **C. Fröhlich, W. Kemmetmüller, and A. Kugi**

and published in *Mathematical and Computer Modelling of Dynamical Systems.*

Contact:

Automation and Control Institute (ACIN)
Vienna University of Technology
Gusshausstrasse 27-29/E376
1040 Vienna, Austria

Internet: www.acin.tuwien.ac.at
E-mail: office@acin.tuwien.ac.at
Phone: +43 1 58801 37601
Fax: +43 1 58801 37699

ORIGINAL ARTICLE

Control-oriented modeling of servo-pump driven injection molding machines in the filling and packing phase

C. Froehlich[a], W. Kemmetmüller[a] and A. Kugi[a]

[a]Automation and Control Institute, TU Wien, Gußhausstraße 27-29/E376, Vienna 1040, Austria

ARTICLE HISTORY
Compiled May 14, 2018

Abstract
Servo-valves or variable displacement pumps are typically used to control conventional hydraulic injection molding machines. Recent developments in electrical drive technology allow to utilize servo-motor driven pumps instead, which is beneficial due to their higher energy efficiency. Their dynamic behavior, however, is significantly different compared to the conventional setup. Thus, currently used mathematical models and control concepts cannot be directly applied. This paper presents a computationally efficient and scalable mathematical model of the injection process for these servo-pump driven injection molding machines. A first-principles model of the injection machine is combined with a phenomenological model describing the injection process, i. e., the compression of the melt and the polymer flow into the mold. The proposed model is tailored to real-time applications and serves as an ideal basis for the design of model-based control strategies. The feasibility of the proposed model is demonstrated by a number of different experiments. They confirm a high model accuracy over the whole operating range for different mold geometries.

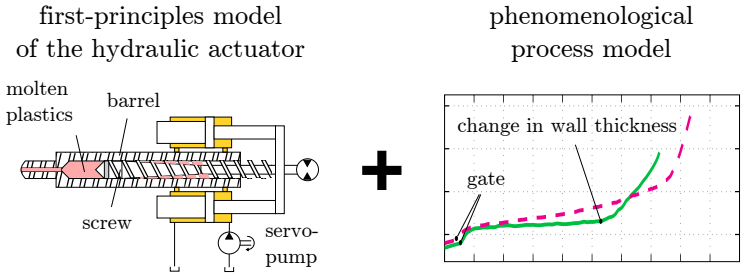

KEYWORDS
control-oriented modeling; injection molding; hydraulic direct drive; first-principles modeling; fluidic systems; non-Newtonian flow; phenomenological process model;

1. Introduction

Injection molding is one of the most important manufacturing processes for the production of goods made of polymer. The injection molding process is cyclic and consists of the following phases: First, the mold is closed with a specific force. Then, the molten

CONTACT C. Froehlich. Email: froehlich@acin.tuwien.ac.at

Post-print version of the article: C. Fröhlich, W. Kemmetmüller, and A. Kugi, "Control-oriented modeling of servo-pump driven injection molding machines in the filling and packing phase", *Mathematical and Computer Modelling of Dynamical Systems*, vol. 24, pp. 451–474, 2018. DOI: 10.1080/13873954.2018.1481870

polymer is injected into the mold by a reciprocating screw. To completely fill the mold and to account for the shrinking of the polymer during cooling, a high pressure is applied to the polymer during the packing phase. Before the next cycle starts, the screw is rotated and feeds cold polymer granulate from a hopper to the front of the screw. The pressure applied to the screw causes a shearing and melting of the granulate to a homogeneous melt in front of the screw. After the cooling time of the part has passed, the mold is opened and the final part is ejected. See, e. g., [1] for a more detailed description.

An accurate control of the process variables (e. g. injection pressure and speed) to their desired values (in particular during the filling and packing phase) is essential to ensure a constant high product quality. An accurate mathematical description of the dynamic system behavior is an important prerequisite for the design and test of control strategies. This work, thus, aims at developing a control-oriented mathematical model of (servo-pump driven) hydraulic injection molding machines (IMM) in the filling and packing phase. For this, the following conditions should be taken into account:

(i) Even though the mechanical construction of a specific IMM is well known, there is a large variety of construction sizes and variants. The mathematical model should be easily adaptable to these variants without the need for excessive calibration by measurements. Thus, a physics-based modeling approach is utilized, where special care is taken that as many model parameters as possible can be directly calculated from construction parameters. This also allows to easily transfer the model-based control strategies to different construction sizes of a machine.

(ii) In contrast, there is typically only very limited knowledge of the mold, when the controller of an IMM is designed. It is well documented in the literature that an accurate modeling of the flow of polymer in the complex geometries of molds (flow of non-Newtonian fluids, combined continuum mechanics and thermodynamics problem) is rather difficult. As will be discussed in the next section, typically finite-element models are utilized which require a detailed knowledge of the mold geometry and the polymer behavior. The exact knowledge of the flow of material in the mold is not of primary interest for the control of the IMM and thus not considered in this work. Instead, a heuristic approach is proposed to obtain a model which describes the flow of polymer into the mold as a function of the injection pressure and the filling level of the mold.

(iii) The resulting model should be computationally inexpensive while describing the most important dynamic effects and nonlinearities encountered during the injection process.

The paper is organized as follows: Section 2 gives a detailed overview of the existing literature for modeling the injection process and injection molding machines. The derivation of the mathematical model of the injection unit and the process model (model of the mold) is introduced in Section 3. A comparison of simulation and measurement results is presented in Section 4 to evaluate the overall model performance.

2. Literature Survey

The mathematical modeling of the injection molding process has been an active field of research in the last decades. The main focus of these works is in the field of modeling the constitutive behavior of polymer and their flow into a mold. E. g., Spencer and Gilmore [2] investigated the basic phenomena which occur during injection molding

Post-print version of the article: C. Fröhlich, W. Kemmetmüller, and A. Kugi, "Control-oriented modeling of servo-pump driven injection molding machines in the filling and packing phase", *Mathematical and Computer Modelling of Dynamical Systems*, vol. 24, pp. 451–474, 2018. DOI: 10.1080/13873954.2018.1481870
The content of this post-print version is identical to the published paper but without the publisher's final layout or copy editing.

in the early 1950s. Several authors have followed this research up to today [3–6]. The theoretical findings have been implemented in a number of commercial simulation tools, which are mainly used for designing molds. The underlying modeling approaches typically rely on computational fluid dynamics methods (CFD), which require the accurate knowledge of the mold geometry and of the polymer properties. Their high computational costs make them unsuitable for controller design.

Abu Fara [7] published an analysis of the dynamics of the injection molding process. Step response tests were conducted to fit black-box transfer functions for the packing phase as well as pseudo-static relationships for the filling phase. Wang [8] proposed a 4^{th}-order transfer function for controller synthesis, which was also used later on by other authors [9, 10]. Kamal et al. [11] designed a simple controller based on a first-order-plus-deadtime approximation of the pressure dynamics. This type of transfer functions has been widely used for control design [12–15]. Similar transfer function models for IMM can also be found in [16–22]. Alternative approaches are based on parametric models like ARX-[23, 24], ARMAX-[25], CARMA-[26], or CARIMA-[27] models or different time-series models [28, 29]. While these black-box models are quite simple and facilitate the design of linear controllers, they only describe the system dynamics for a specific setting at a certain operating point.

Another approach to model and control the dynamics of the injection process without utilizing first-principles models are neural networks (NN). Petrova and Kazmer combined a NN with process knowledge for the training of the NN and derived a process model for the injection pressure [30]. Michaeli and Schreiber developed a NN for cavity pressure control enabling a model-based predictive control of process variables [31]. NN have also been proposed for the modeling of further product properties, such as the tensile modulus [32]. The main drawback of NN is that their quality depends on a vast amount of training data for a specific injection molding machine. Thus, these models are neither scalable nor easily transferable to different construction sizes and therefore do not meet the requirements given in Section 1.

To reduce the computational costs and to (at least approximately) take into account the physics of the injection process, a number of lumped-parameter models have been introduced in the literature. Shankar and Paul [33] utilize a laminar flow resistance for each melt flow passage in the mold combined with a simple hydraulic actuator model. During the packing phase, the time evolution of the melt pressure is considered by two cavities, i. e., the mold cavity and the antechamber in front of the screw. This two-cavity approach is widely used, see, e. g., [34–36]. Rafizadeh et al. [37, 38] proposed separate models for the filling and the packing phase with a power law for the pressure drop along the flow path. Chiu et al. [39] and Woll and Cooper [40] derived simplified models by considering the mold geometry in form of the momentum balance and the shear force of the polymer flow together with a simple actuator model. Cho et al. [41] and Lin and Cheng [42] extended these models by making the flow resistance dependent on the melt front position. Daxberger et al. [43] derived a spatially distributed one-dimensional model for the flow path, but reduced the overall model to a 2^{nd}-order lumped-parameter model for the controller design, where the mold specific parameters are estimated online. Dorner et al. [44] proposed a pseudo-static pressure drop during the filling phase and a one-cavity model for the packing phase. All these models have in common that they are only applicable if the gate, runner, sprue and mold geometry is accurately known and can be approximated by simple shapes.

To account for this problem, Zheng and Alleyne [45] used a power law for the volume flow into the mold, where the constant parameters are determined empirically, together with a two-cavity model. Reiter et al. [46] derived a model for the packing phase,

Post-print version of the article: C. Fröhlich, W. Kemmetmüller, and A. Kugi, "Control-oriented modeling of servo-pump driven injection molding machines in the filling and packing phase", *Mathematical and Computer Modelling of Dynamical Systems*, vol. 24, pp. 451–474, 2018. DOI: 10.1080/13873954.2018.1481870

where the melt pressures within the antechamber and the mold cavity are determined by the static polymer's equation of state. A simple model for the evolution of the melt temperature is proposed and the pressure drop is described by a valve equation with a time-dependent empirically determined flow coefficient.

While the latter models still demand at least some basic knowledge of the mold, e. g., the mold cavity volume, data-based models for describing the influence of the injection process on the injection unit can be formulated without any specific knowledge of the mold. For instance, Tan et al. [47] introduced a dynamic model of the melt pressure inside the barrel with a constant volume flow into the mold during the filling phase. Another dynamic model for the packing phase, where the overall response of the mold is modeled as an empirically determined position-dependent force acting on the screw, can be found in [48].

In the present work, a phenomenological model of the injection process will be proposed as well, which has some similarities to the latter models, but is capable of describing both the filling and the packing phase with one model. It will be shown by measurements that the proposed model is able to accurately capture the behavior of different mold geometries without the need for excessive calibration.

The focus of the literature review given so far is on the modeling of the injection process, where the injection molding machine, i. e., the dynamics of the injection actuators, is, if at all, only incorporated by very simplified mathematical models. The dynamics of the actuation system can become an important factor in particular for the considered hydraulically actuated IMM. Hydraulic injection machines considered in the literature typically include hydraulic pumps running at constant speed and servo-valves for the control. For instance, Shankar and Paul [33] used a machine with a constant hydraulic oil volume flow and a pressure relief valve. Alternatively, servo-valves were used as flow control valves and the systems were typically modeled with constant supply pressure [7, 36, 39, 41, 45, 48–51]. Some manufacturers use variable displacement pumps instead of servo-valves [52].

In this work, a servo-drive-based injection molding machine is considered, where the system is controlled by adjusting the speed of a servo-motor. For this specific design, only a very few publications can be found. Wang et al. [53] discussed the usage of the pump speed as control input and Peng et al. [54] introduced a model, where the dynamics of the servo-drive is modeled in combination with a simple hydraulic system. The goal of the present paper is to derive a detailed physics-based model of the servo-drive-based injection molding system and combine it with a phenomenological process model. The commonly used simple hydraulic models, cf. [53, 54], are improved in a way of systematically considering cavitation of the hydraulic fluid, which can occur in certain parts of the hydraulic system. The validation of the resulting overall model (including the process model) by measurement results will show a high model accuracy at low computational costs.

3. System Model

Figure 1 gives an overview of the relevant components of the considered hydraulic injection unit for the filling and packing phase. Molten polymer is pushed from the antechamber through the nozzle into the mold by moving the (non-rotating) reciprocating screw to the left. The non-return valve prevents a back flow of the melt if the screw is moved forward. During the injection phase, i. e., the forward movement of the screw, the screw does not rotate to ensure a proper closing of the non-return valve.

Post-print version of the article: C. Fröhlich, W. Kemmetmüller, and A. Kugi, "Control-oriented modeling of servo-pump driven injection molding machines in the filling and packing phase", *Mathematical and Computer Modelling of Dynamical Systems*, vol. 24, pp. 451–474, 2018. DOI: 10.1080/13873954.2018.1481870

The screw is moved axially by means of the hydraulic cylinders. The force and thus the motion of the pistons is controlled by the mass flow of hydraulic oil into and out of the cylinder chambers. In a classical setup of a hydraulic injection machine, a directional servo-valve is utilized to adjust the mass flow into the injection-side chamber of the hydraulic cylinder while the supply pressure is controlled by means of the displacement/speed of the pump or by a pressure control valve. In the considered servo-pump injection molding system, however, the mass flow into the injection-side chamber is directly controlled by means of the rotational speed of a fixed displacement pump. The servo-valve is completely opened in this setup and not utilized for the control[1]. The pump is driven by a speed-controlled servo-drive, which allows a fast adjustment of the rotational speed of the pump. The return chamber of the injection cylinder is connected to the tank and the plastication drive is not active during the filling and packing phase.

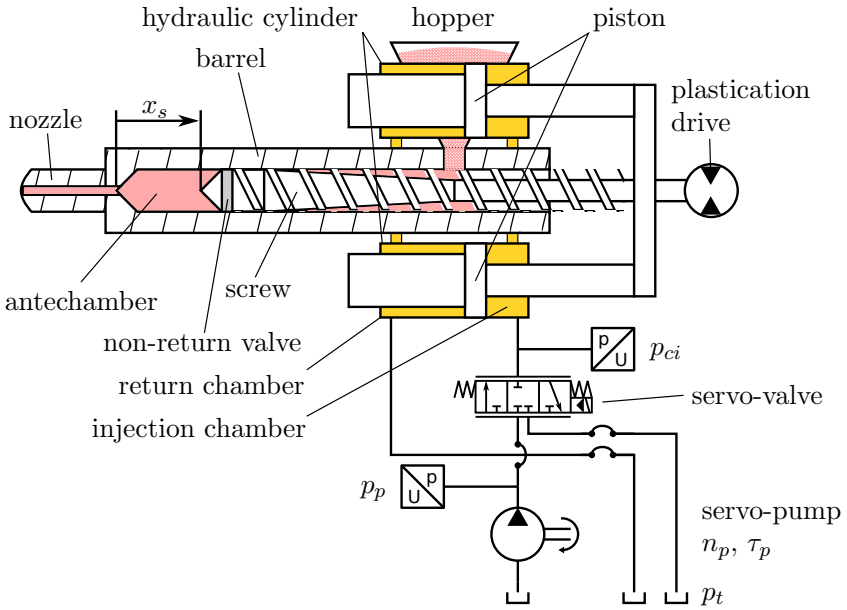

Figure 1.: Overview of the hydraulic injection unit.

The overall mathematical model consists of models of the mechanical and hydraulic subsystem of the IMM and a phenomenological model of the mold.

3.1. *Mechanical Subsystem*

The overall force acting on the hydraulic pistons is given by

$$F_{tot} = A_{ac}(p_{ac} - p_0) - 2A_{ci}(p_{ci} - p_0) - F_{fr}, \tag{1}$$

where p_{ac} is the melt pressure in the antechamber, A_{ac} is the cross-sectional area of the screw, p_{ci} is the hydraulic pressure in the injection (right) chamber of the cylinder (area A_{ci}). The return (left) chamber is connected to the tank with pressure p_t. Subsequently, the tank pressure p_t is assumed to be identical to the ambient pressure

[1]Since the valve cannot be taken out in the considered experimental setup, the influence of the valve (i. e. the pressure drop) is taken into account in the subsequent mathematical model.

Post-print version of the article: C. Fröhlich, W. Kemmetmüller, and A. Kugi, "Control-oriented modeling of servo-pump driven injection molding machines in the filling and packing phase", *Mathematical and Computer Modelling of Dynamical Systems*, vol. 24, pp. 451–474, 2018. DOI: 10.1080/13873954.2018.1481870

p_0, i. e., $p_t = p_0 = \text{const}$. Hence, the pressure in the return chamber does not contribute to the overall force[2]. $F_{fr} = F_{fr,c} + F_{fr,s}$ is the sum of the friction force $F_{fr,c}$ in the hydraulic cylinder and the friction force $F_{fr,s}$ between the screw and the barrel. For $F_{fr,c}$, a static friction model of the form

$$F_{fr,c} = d_v v_s + d_q v_s |v_s| + d_c \tanh\left(\frac{v_s}{v_{t0}}\right) \tag{2}$$

is utilized, with the velocity $v_s = \dot{x}_s$ of the screw, the viscous friction coefficient d_v, the quadratic friction coefficient d_q, the Coulomb friction coefficient d_c and the reference velocity v_{t0}.

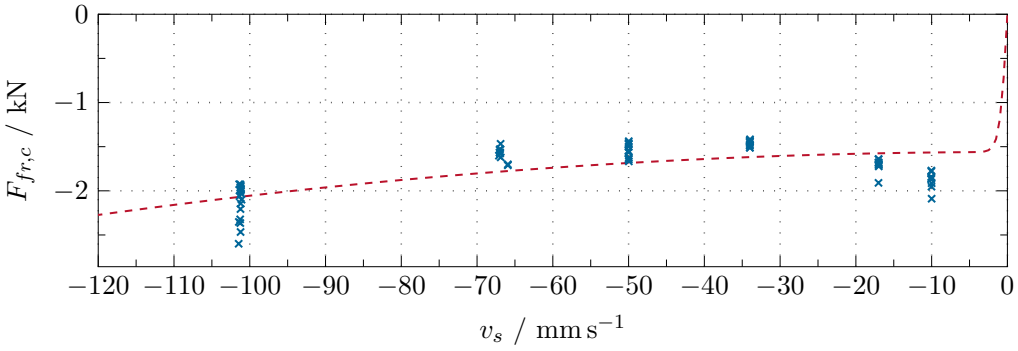

Figure 2.: Comparison of the measured friction force with the model $F_{fr,c}(v_s)$ from (2).

Figure 2 shows a comparison of the model $F_{fr,c}$ from (2) with measurements on the test stand. It can be seen that the basic characteristics is well approximated, in particular if one takes into account that the friction shows significant variations due to other influencing factors. However, for very low speed of the screw some kind of Stribeck effect, i. e., an increase of the friction force with decreasing velocity, can be observed, which is not covered by (2). Since the resulting error is small in practically relevant scenarios, this effect is neglected.

The friction force $F_{fr,s}$ describes the resistance due to the flow of molten polymer between the screw and the barrel when the barrel is filled with partially melted polymer. It is described by

$$F_{fr,s} = d_s \operatorname{sgn}(v_s) |v_s|^n. \tag{3}$$

Therein, non-Newtonian flow behavior of polymer is taken into account by the flow behavior index n, with $0 < n < 1$ for shear-thinning materials. The friction parameter d_s is approximated by

$$d_s = \tilde{d}_s (l_0 - x_s) A_{ac}, \tag{4}$$

with an experimentally determined parameter $\tilde{d}_s$ and the length l_0 of the wetted cylinder surface, i. e., the screw, at $x_s = 0$.

[2]The pressure drop in the return line results in a velocity-dependent pressure in the return chamber of the cylinder. This additional force is included in the friction model (2) such that no extra return line model is required.

Post-print version of the article: C. Fröhlich, W. Kemmetmüller, and A. Kugi, "Control-oriented modeling of servo-pump driven injection molding machines in the filling and packing phase", *Mathematical and Computer Modelling of Dynamical Systems*, vol. 24, pp. 451–474, 2018. DOI: 10.1080/13873954.2018.1481870
The content of this post-print version is identical to the published paper but without the publisher's final layout or copy editing.

The balance of momentum of the screw and cylinder piston with the overall mass m_s is given by

$$m_s \frac{\mathrm{d}}{\mathrm{d}t} v_s = \begin{cases} 0\,, & x_s = x_s^{stop},\ F_{tot} \leq 0 \\ F_{tot}\,, & \text{else,} \end{cases} \tag{5}$$

where x_s^{stop} is the mechanical end stop at the very left side of the cylinder. It is assumed that the whole kinetic energy is dissipated when the system reaches this end stop, i. e., $v_s = 0$ is set.

3.2. *Hydraulic Subsystem*

In this subsection, the hydraulic actuation system for the mechanical reciprocating screw is modeled. The main parts of the hydraulic system are the servo-pump and the hydraulic cylinder.

3.2.1. Isentropic Fluid Model of the Hydraulic Oil

In the considered system, the hydraulic oil can reach pressures up to 200 bar (e. g. in the cylinder chamber), while in other parts the pressure can drop below ambient pressure p_0 for certain operating conditions[3]. Thus, a model which accounts for the significant change of the mass density ϱ and the bulk modulus β as a function of p,

$$\frac{\partial \varrho(p)}{\partial p} = \frac{\varrho(p)}{\beta(p)}, \tag{6}$$

and which takes into account the cavitation effect for pressures below p_0, is required. In [55–57], a phenomenological fluid model is described, which divides the pressure range into the following three parts:

(1) $p \geq p_{vap,u}$: For pressures above the upper vapor pressure $p_{vap,u}$ the oil is liquid. Here, the model takes into account the increase of β and ϱ with respect to the pressure p.
(2) $p_{vap,l} < p < p_{vap,u}$: In this pressure range, the oil starts to vaporize, i. e., a mixture of vaporized and liquid oil is present. Here, the effective bulk modulus and density for the mixture is calculated.
(3) $p \leq p_{vap,l}$: Below the lower vapor pressure the oil is vaporized entirely. In this region, the oil is described by the ideal gas equation.

A detailed description of the model is given in [55–57]. The fluid model ensures physically meaningful pressures (no pressures below 0) and makes sure that the balance of mass holds. The resulting model is shown in Figure 3 for the liquid phase and Figure 4 for pressures below ambient pressure p_0.

[3]This can occur in the following two cases: (i) If the servo-pump is accelerated very fast, cavitation (i. e., pressures below ambient pressure) occurs due to the inertia of the hydraulic fluid in the connection from the tank to the pump. (ii) If the hydraulic cylinders are moving with high velocity and the servo-pump is decelerated rapidly, the inertia of the overall moving mass can also cause cavitation. Nevertheless, these operating conditions should be avoided to reduce wear of the servo-pump.

Post-print version of the article: C. Fröhlich, W. Kemmetmüller, and A. Kugi, "Control-oriented modeling of servo-pump driven injection molding machines in the filling and packing phase", *Mathematical and Computer Modelling of Dynamical Systems*, vol. 24, pp. 451–474, 2018. DOI: 10.1080/13873954.2018.1481870

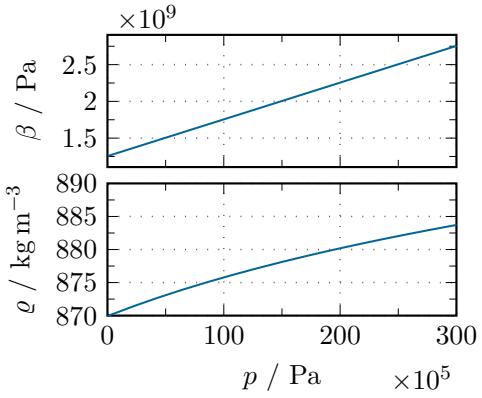

Figure 3.: Density ϱ and bulk modulus β of oil in the liquid phase.

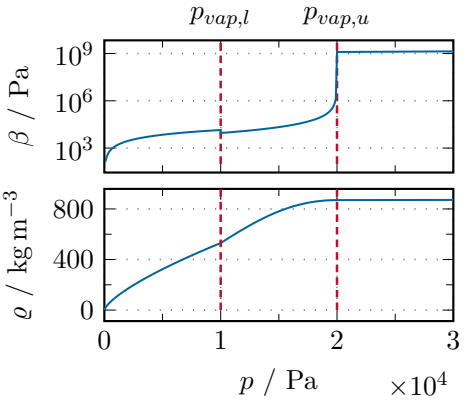

Figure 4.: Density ϱ and bulk modulus β of oil in the vapor phase.

Post-print version of the article: C. Fröhlich, W. Kemmetmüller, and A. Kugi, "Control-oriented modeling of servo-pump driven injection molding machines in the filling and packing phase", *Mathematical and Computer Modelling of Dynamical Systems*, vol. 24, pp. 451–474, 2018. DOI: 10.1080/13873954.2018.1481870

3.2.2. Servo-Pump

The hydraulic system is supplied and controlled by an internal gear pump attached to a servo-drive. The mass flow $\dot{m}_p$ generated by the pump is given by

$$\dot{m}_p = -\varrho_p V_{th} n_p \eta_{vol}, \tag{7}$$

with the pump speed n_p, the volumetric efficiency η_{vol}, and the theoretical geometrical displacement volume V_{th}. The mass density $\varrho_p(p)$ is given by the constitutive equation (6) of Section 3.2.1, where $p = p_t$ is used for $\dot{m}_p \geq 0$ and $p = p_p$ for $\dot{m}_p < 0$. The dependency of the volumetric efficiency η_{vol} on the pump pressure p_p can be well approximated by

$$\eta_{vol} = \eta_{vol0} - (\eta_{vol0} - \eta_{voln}) \left(\frac{p_p - p_t}{p_{voln} - p_t} \right)^2, \tag{8}$$

with the nominal efficiency η_{vol0} at $p_p = p_t$ and the decreased efficiency η_{voln} at $p_p = p_{voln}$. The hydromechanic pump torque $\tau_{p,hm}$ is given by

$$\tau_{p,hm} = \frac{\tau_p}{\eta_{hm}} = -\frac{V_{th}}{2\pi} \frac{(p_p - p_t)}{\eta_{hm}}, \tag{9}$$

with the pressure-dependent hydromechanic efficiency η_{hm}. A polynomial function $\eta_{hm}(p_p)$ is again utilized to approximate measurements.

The balance of angular momentum for the pump rotational speed n_p yields

$$\frac{\mathrm{d}}{\mathrm{d}t} n_p = \frac{1}{2\pi J_p} (-\tau_{p,hm} - \tau_{fr} + \tau_{el}), \tag{10}$$

with the momentum of inertia J_p, the electric drive torque τ_{el}, and the friction torque

$$\tau_{fr} = \operatorname{sgn}(n_p) d_{c,mot} + n_p d_{v,mot} \ . \tag{11}$$

Measurements confirm that the friction torque can be accurately approximated by (11). As discussed before, the speed of the pump is controlled by a subordinate speed control loop implemented on the inverter, which uses the electric drive torque τ_{el} as control input. The inverter exhibits remarkable dead-time behavior, resulting from communication delays and internal interpolation algorithms. For the injection process, the subordinate pump speed control loop is assumed to be ideal but with an input dead-time t_{dt}, which is why the delayed desired pump speed $n_p^d(t - t_{dt})$ serves as new control input. The ODE (10) is an important part of the model to calculate the required electric torque τ_{el}.

3.2.3. Evolution of the Injection and Pump Pressure

The screw is actuated by two parallel double-acting cylinders, where the respective chambers are hydraulically connected. As described before, the return chambers are assumed to be connected to tank with pressure $p_t = p_0$. Thus, only the injection chamber is modeled in form of one effective cylinder with the corresponding doubled

Post-print version of the article: C. Fröhlich, W. Kemmetmüller, and A. Kugi, "Control-oriented modeling of servo-pump driven injection molding machines in the filling and packing phase", *Mathematical and Computer Modelling of Dynamical Systems*, vol. 24, pp. 451–474, 2018. DOI: 10.1080/13873954.2018.1481870

volume and area. The balance of mass for the injection chambers reads as

$$\frac{\mathrm{d}}{\mathrm{d}t}p_{ci} = \frac{\beta_{ci}}{2(V_{ci0} - A_{ci}x_s)}\left(\frac{\dot{m}_{sv}}{\varrho_{ci}} + 2A_{ci}v_s\right). \tag{12}$$

Here, p_{ci} denotes the pressure in the injection chamber and ϱ_{ci} and β_{ci} are the corresponding mass density and the bulk modulus given by the fluid model introduced in Section 3.2.1. A_{ci} is the piston area and V_{ci0} the chamber volume for $x_s = 0$.

The mass flow $\dot{m}_{sv}$ of the servo-valve, which is placed in front of the injection chamber in the present setup, can be described by $\dot{m}_{sv} = \dot{m}_{sv,pc} - \dot{m}_{sv,ct}$, with

$$\dot{m}_{sv,pc} = \alpha_{sv}\sqrt{2\varrho_{sv,pc}(p_{pc})}A_{sv,pc}(x_{sv})\sqrt{|p_p - p_{ci}|}\,\mathrm{sgn}(p_p - p_{ci}) \tag{13a}$$

$$\dot{m}_{sv,ct} = \alpha_{sv}\sqrt{2\varrho_{sv,ct}(p_{ct})}A_{sv,ct}(x_{sv})\sqrt{|p_{ci} - p_t|}\,\mathrm{sgn}(p_{ci} - p_t). \tag{13b}$$

Therein, α_{sv} is the contraction coefficient, p_p the pump pressure, and $A_{sv,pc}$, $A_{sv,ct}$ are the opening areas of the valve from supply to chamber (pc) and from chamber to tank (ct), respectively, which can be changed by the valve position x_{sv}. The pressure for calculating the density $\varrho_{sv,pc}(p_{pc})$ depends on the direction of the flow. Thus, for $\dot{m}_{sv,pc} \geq 0$, the pressure $p_{pc} = p_p$ before the valve is used, while $p_{pc} = p_{ci}$ for $\dot{m}_{sv,pc} < 0$. Analogously, $p_{ct} = p_{ci}$ is used for $\varrho_{sv,ct}(p_{ct})$ for $\dot{m}_{sv,ct} \geq 0$ and $p_{ct} = p_t$ for $\dot{m}_{sv,ct} < 0$.

Remark 1. Since the servo-valve is completely opened in the considered scenarios, the servo-valve dynamics is not further discussed in this paper. It is assumed that the servo-valve position x_{sv} is ideally controlled.

The pump pressure is assumed to be uniform within the supply line from the pump to the valve and is described by the balance of mass

$$\frac{\mathrm{d}}{\mathrm{d}t}p_p = \frac{\beta_p}{V_p\varrho_p}(\dot{m}_p - \dot{m}_{sv,pc}), \tag{14}$$

with the volume V_p of the supply line and $\dot{m}_p$ from (7). The bulk modulus β_p and the mass density ϱ_p are given by the fluid model of Section 3.2.1.

Remark 2. The effective bulk modulus describes the apparent compressibility of the fluid in a hydraulic cavity, combining the compressibility of the oil and the stiffness of the hydraulic cavity. Due to the usage of flexible hydraulic hoses in the supply line the fluid model parameters for the bulk modulus β_p can be different from those of β_{ci} and may be identified by means of measurements.

3.3. *Process Model*

The process model summarizes the description of the molten polymer in the antechamber and the mass flow into the mold.

Post-print version of the article: C. Fröhlich, W. Kemmetmüller, and A. Kugi, "Control-oriented modeling of servo-pump driven injection molding machines in the filling and packing phase", *Mathematical and Computer Modelling of Dynamical Systems*, vol. 24, pp. 451–474, 2018. DOI: 10.1080/13873954.2018.1481870

3.3.1. Antechamber

The antechamber of the IMM is filled with molten polymer before the filling process starts, see Figure 5. The volume V_{ac} of the antechamber is given by

$$V_{ac} = A_{ac}(x_{s0} + x_s + r_s p_{ac}) \ , \tag{15}$$

where $A_{ac} = D_s^2\pi/4$ is the cross-sectional area of the screw with diameter D_s and $A_{ac}x_{s0}$ accounts for the dead volume remaining for $x_s = 0$. The pressure p_{ac} of the polymer in the antechamber yields a deformation of the screw due to its flexibility. This effect is taken into account by the stiffness coefficient r_s.

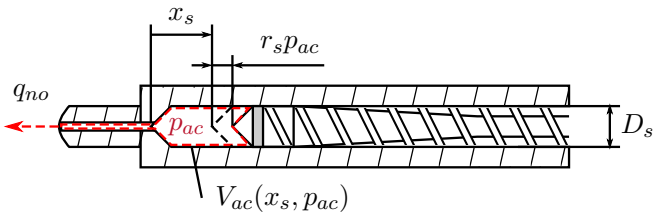

Figure 5.: Melt cushion model.

The conservation of mass applied to the antechamber reads as

$$\frac{\mathrm{d}}{\mathrm{d}t} m_{ac} = \frac{\mathrm{d}}{\mathrm{d}t}(\varrho_{ac}(p_{ac}, T_{ac})V_{ac}(x_s, p_{ac})) = -\varrho_{ac} q_{no}, \tag{16}$$

where q_{no} denotes the volume flow into the mold [4].

The density ϱ_{ac} of the polymer is a function of the pressure p_{ac} and the temperature T_{ac}. One common heuristic model is the modified two-domain Tait equation, see, e. g., [6]. It describes the specific volume $v_{ac} = 1/\varrho_{ac}$ as a function of the temperature T_{ac} and pressure p_{ac} in the form

$$v_{ac}(p_{ac}, T_{ac}) = v_0(T_{ac})\left(1 - c_1 \ln\left(1 + \frac{p_{ac}}{B(T_{ac})}\right)\right) + v_T(p_{ac}, T_{ac}) \ , \tag{17}$$

with the constant c_1 and

$$v_0(T_{ac}) = b_1 + b_2(T_{ac} - b_5) \tag{18a}$$
$$B(T_{ac}) = b_3 \exp(-b_4(T_{ac} - b_5)) \ . \tag{18b}$$

The term $v_T(p_{ac}, T_{ac})$ accounts for the change in the specific volume of semi-cristalline materials when changing their structure from cristalline to amorph during melting

$$v_T(p_{ac}, T_{ac}) = \begin{cases} b_7 \exp(b_8(T_{ac} - b_5) - b_9 p_{ac}), & T_{ac} \le T_t \\ 0, & T_{ac} > T_t \end{cases} \tag{19}$$

with the transition temperature $T_t = b_5 + b_6 p_{ac}$. The constant parameters $b_i, i = 1, \ldots, 9$ characterize the different materials and can be found in the literature or in commercial databases as, e. g., included in Autodesk Moldflow®.

[4] During the filling and packing phase, which are considered in this paper, the non-return valve at the screw is closed. Small leakages due to a possible imperfect closing of the valve are subsumed in the volume flow q_{no}.

Post-print version of the article: C. Fröhlich, W. Kemmetmüller, and A. Kugi, "Control-oriented modeling of servo-pump driven injection molding machines in the filling and packing phase", *Mathematical and Computer Modelling of Dynamical Systems*, vol. 24, pp. 451–474, 2018. DOI: 10.1080/13873954.2018.1481870
The content of this post-print version is identical to the published paper but without the publisher's final layout or copy editing.

Remark 3. While the Tait model can give an accurate description of the material behavior in a wide temperature and pressure range, it strongly relies on the knowledge of the model parameters $b_i, i = 1, \ldots, 9$ and thus on the polymer used. In most of the cases, these data are not provided by the operator of the machine and thus are not available for a control strategy. In these cases, it is necessary to use simpler material models. Given the fact that the temperature of the polymer is basically constant in the considered filling and packing phase, its influence can be neglected and the pressure-dependent bulk modulus β_{ac} is approximated in the form

$$\beta_{ac} = \beta_0 + \beta_1 p_{ac} + \beta_2 p_{ac}^2. \tag{20}$$

The parameters β_i, $i = 0, 1, 2$, have to be identified from measurements, e. g., during the packing phase.

Inserting the material model (either (17) with (6) or (20)) into (16) and considering (15) yields

$$\frac{\mathrm{d}}{\mathrm{d}t} p_{ac} = \frac{\beta_{ac}}{x_{s0} + x_s + r_s(p_{ac} + \beta_{ac})} \left(-v_s - \frac{q_{no}}{A_{ac}} \right), \tag{21}$$

where the temperature T_{ac} is assumed to be constant and $v_s = \dot{x}_s$.

Before the start of the filling phase (after the plastication phase), the screw is pulled back to decompress the melt completely and open the non-return valve. This is done to increase the repeatability of the process. In this case, $p_{ac} = p_0$ is given at the beginning of the filling phase until the screw touches the melt at the position $x_s = x_{s,f0}$, i. e.,

$$\frac{\mathrm{d}}{\mathrm{d}t} p_{ac} = \begin{cases} 0\,, & x_s > x_{s,f0} \\ \mathrm{RHS}((21))\,, & \text{else}\ . \end{cases} \tag{22}$$

3.3.2. Mass flow into the Mold

Modeling the filling of the mold with liquid polymer is a difficult task, in particular since the coupled thermodynamic and fluid mechanics problem has to be solved for complex mold geometries. Typically, specialized CFD simulations are used for this task, which, however, require accurate knowledge of the mold geometry and are computationally complex, cf. [6]. These models are not suitable for the design of control strategies or for fast transient simulations.

Therefore, in this work, a simplified approach is proposed which aims at finding a semi-heuristic approximation of the volume flow q_{no}. This model should be capable of representing the main dynamic behavior and being parameterized by measurements without the need of an accurate knowledge of the mold geometry.

For this task, the process is split into two parts: In the filling phase, the mold is filled with liquid polymer, where q_{no} is a function of the pressure p_{ac} and the filling level of the mold, which is basically equivalent to the screw position x_s. In the subsequent packing phase, the mold is completely filled and a volume flow q_{no} into the mold only occurs due to elastic deformation of the polymer (if there are changes in the pressure p_{ac}) and the shrinking of the polymer due to cooling. Since the cooling is basically a function of time, the shrinking of the polymer can be described as a function of time as well.

Post-print version of the article: C. Fröhlich, W. Kemmetmüller, and A. Kugi, "Control-oriented modeling of servo-pump driven injection molding machines in the filling and packing phase", *Mathematical and Computer Modelling of Dynamical Systems*, vol. 24, pp. 451–474, 2018. DOI: 10.1080/13873954.2018.1481870

Based on this discussion, the volume flow q_{no} into the mold is approximated by the Ostwald-de Waele model [6, 58] in the form

$$q_{no} = A_{no}\left(\frac{p_{ac} - p_0}{r_{no}}\right)^{1/n}. \tag{23}$$

Here, A_{no} is the cross-sectional area of the nozzle, n is the polymer flow behavior index, and r_{no} is the filling resistance [45].

To account for the different behavior in the filling and packing phase, the filling resistance is defined as follows: In the filling phase, the resistance r_{no} is given as a function of x_s, i. e., $r_{no} = r_{no,x}(x_s)$, which can be identified from measurements of the injection molding machine with the considered mold. The filling phase starts at $x_s = x_{s,f0}$ and ends when the form is completely filled at $x_s = x_{s,fe}$. If the overall volume V_{mo} of the mold is known, then $x_{s,fe}$ can be approximated by $x_{s,fe} = x_{s,f0} - V_{mo}/A_{ac} = x_{s,f0} - \Delta x_{s,mo}$, where $\Delta x_{s,mo}$ is the displacement of the screw required to fill the mold.

Remark 4. In cases where the mold volume is not accurately known, another possibility to define $x_{s,fe}$ is as follows: Typically, the pressure p_{ac} required to fill a mold with constant volume flow q_{no} shows a steep rise when the mold is close to complete filling. Defining a characteristic pressure limit, the position $x_{s,fe}$ is reached when p_{ac} exceeds this limit.

In the packing phase, the resistance $r_{no} = r_{no,t}(t)$ is approximated by the following heuristic model

$$r_{no,t}(t) = \left(r_{no,x}(x_{s,fe}) + r_{fz}\left(1 - \mathrm{e}^{\left(-\frac{t-t_{fe}}{t_{fz1}}\right)}\right)\right)\mathrm{e}^{\left(\frac{t-t_{fe}}{t_{fz2}}\right)}, \tag{24}$$

with the parameters r_{fz}, t_{fz1}, and t_{fz2}, which have to be identified from measurements. In (24), t_{fe} corresponds to the time when $x_s = x_{s,fe}$ holds, i. e., when the mold is completely filled. The overall model for the flow resistance can be summarized as follows

$$r_{no} = \begin{cases} r_{no,x}(x_s), & x_s > x_{s,f0} - \Delta x_{s,mo} \\ r_{no,t}(t), & \text{else.} \end{cases} \tag{25}$$

Measurement results show that this model gives a good approximation of the injection molding process for a large variety of molds. A typical behavior for two different molds, which will be used in the experimental validation in Section 4, is presented in Figure 6. Mold A exhibits a pronounced change in the wall thickness at the gate and in the form, which is reflected in the rapid changes in $r_{no,x}$ in Figure 6(a). Mold B has no change in the wall thickness and a steep rise of $r_{no,x}$ only occurs close to the complete filling of the mold. Moreover, the parts produced with these molds have a rather short cooling time, which can be seen in Figure 6(b), where already after approximately 0.3s the flow resistance $r_{no,t}$ reaches a large value, which corresponds to solid polymer in the mold.

Remark 5. If the type of the processed polymer or its parameters are not known the flow behavior index n has to be identified empirically. Using (21) with (23) and

Post-print version of the article: C. Fröhlich, W. Kemmetmüller, and A. Kugi, "Control-oriented modeling of servo-pump driven injection molding machines in the filling and packing phase", *Mathematical and Computer Modelling of Dynamical Systems*, vol. 24, pp. 451–474, 2018. DOI: 10.1080/13873954.2018.1481870
The content of this post-print version is identical to the published paper but without the publisher's final layout or copy editing.

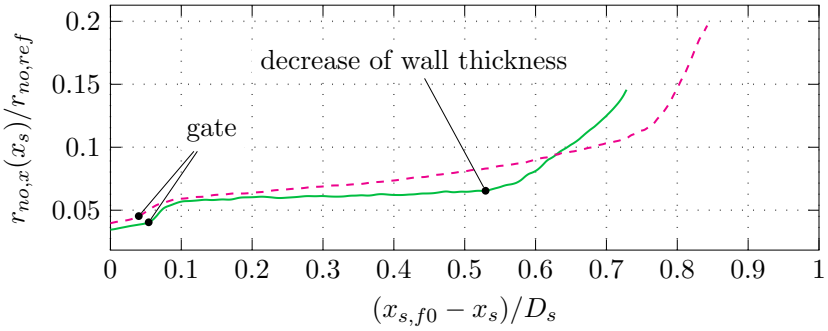

((a)) Filling phase

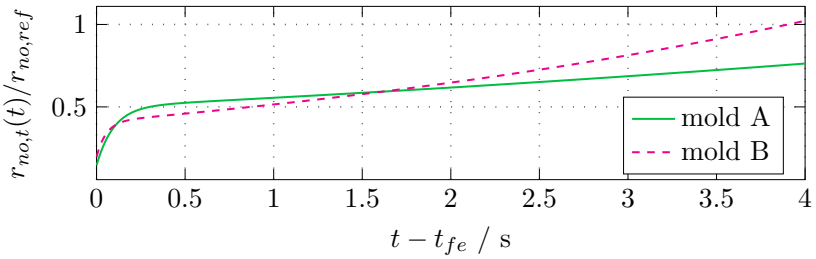

((b)) Packing phase

Figure 6.: Filling resistance r_{no} for two different molds.

choosing segments with the same injection stroke x_s, a constant velocity $\bar{v}_s = \text{const.}$, and constant injection pressure $\bar{p}_{ac} = \text{const.}$, then

$$\bar{v}_s \approx -\frac{A_{no}}{A_{ac}} \left(\frac{\bar{p}_{ac} - p_0}{r_{no,x}(x_s)} \right)^{1/n}$$

approximately holds. Assuming that $r_{no,x}(x_s)$ is independent of the injection velocity, n can be calculated from two measurements with different injection velocities.

4. Experimental Validation

In this section, the proposed mathematical model is validated by a number of measurement results. These measurements were performed on a state-of-the-art injection molding machine (IMM) with its standard PID-based control strategy. The mathematical model of the mechanical and hydraulic subsystem was parametrized by geometry parameters of the specific IMM, for the fluid model nominal parameters were used considering the flexibility of the hydraulic hoses in the supply line, and the friction parameters were identified by measurements according to Figure 2. The parameters $b_i, i = 1, \ldots, 9$ of the Tait equation (17), and the flow behavior index n were taken from literature for the respective material, see, e. g., [59]. The resistance r_{no} of the mold model was calculated from (21) with (23) by means of measurements.

In a first step, the model accuracy of the IMM is investigated without the influence of a specific polymer or the mold geometry. For this so-called dry-run experiment no polymer is inside the barrel. For the simulation results, the measured speed n_p of the pump serves as input. Figure 7 shows the comparison between the measurement and

Post-print version of the article: C. Fröhlich, W. Kemmetmüller, and A. Kugi, "Control-oriented modeling of servo-pump driven injection molding machines in the filling and packing phase", *Mathematical and Computer Modelling of Dynamical Systems*, vol. 24, pp. 451–474, 2018. DOI: 10.1080/13873954.2018.1481870

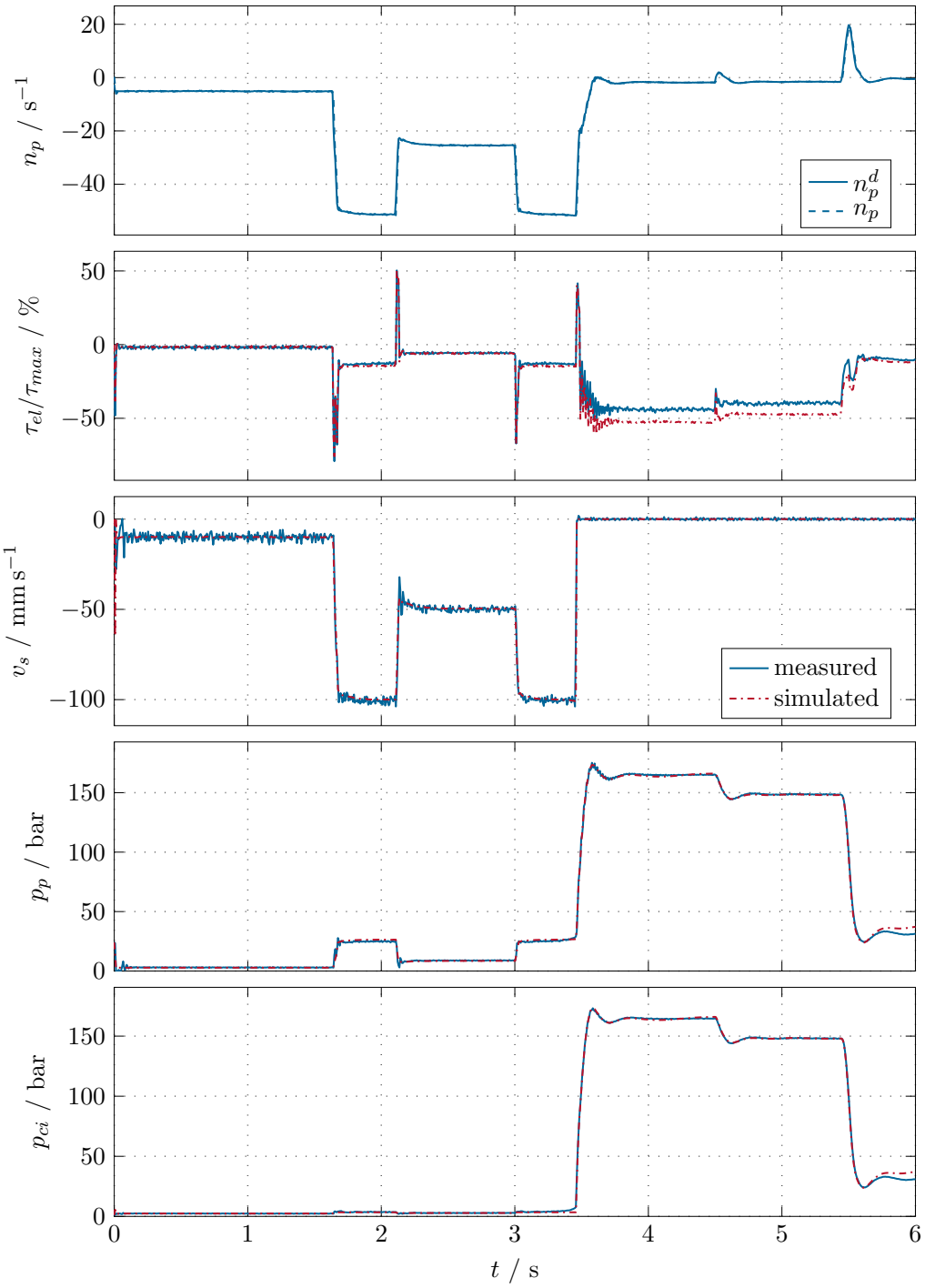

Figure 7.: Validation of the mathematical model for a dry run.

Post-print version of the article: C. Fröhlich, W. Kemmetmüller, and A. Kugi, "Control-oriented modeling of servo-pump driven injection molding machines in the filling and packing phase", *Mathematical and Computer Modelling of Dynamical Systems*, vol. 24, pp. 451–474, 2018. DOI: 10.1080/13873954.2018.1481870

simulation results for the dry-run experiment, where the IMM is velocity controlled with an injection speed profile v_s^d until the screw hits the end stop at $t \approx 3.4\,\mathrm{s}$. From this point on, the IMM is pressure controlled. The measured pump speed n_p shows a good tracking performance of the desired pump speed n_p^d by the pump speed controller. Furthermore, the results clearly confirm that the mathematical model is able to accurately reproduce the time evolution of the measured pump pressure p_s, the cylinder pressure p_{ci}, and the screw velocity v_s.

Additionally, the measured torque τ_{el} is compared to an estimated torque from (10), rearranged for τ_{el} with $\frac{\mathrm{d}}{\mathrm{d}t}n_p$ being calculated numerically. The estimated torque shows a good model accuracy in regions with fast changes of the pump speed. In regions with slower dynamics, low rotational speed and higher pump pressure ($t \approx 3.5\,\mathrm{s}$ to $5.5\,\mathrm{s}$) a higher deviation can be seen. This results from inaccuracies of the pump efficiency η_{hm} in (9). In the control strategy, the torque is an important quantity, since exceeding the torque limits would directly result in large tracking errors of the pump speed. In this context, the accuracy of the predicted torque of the proposed model is high enough.

To analyze the influence of the hydraulic piping system on the overall system dynamics, Figure 8 shows a picture detail of Figure 7. It can be seen that the fast change of the pump speed yields oscillations of the measured pressures in the pipe system, which are not captured by the proposed model. This behavior could be described by adding models for the transmission lines, i. e., the supply and the return line, as proposed by Zheng and Alleyne [45]. A model with sufficient accuracy that captures the whole hydraulic piping system would be rather complex and would thus contradict the desired low model complexity. The experimental results show that the amplitude of the oscillations is rather small and this is only visible due to the small overall pressure levels in the dry-run experiment. In nominal operation (barrel filled with polymer) with significantly larger pressure levels, these oscillations will not have a significant influence on the system performance. Therefore, this effect is not considered in the proposed model.

In order to validate the model of the antechamber, which is filled with liquid polymer, a so-called melt cushion test is performed. In this test scenario, the nozzle is kept closed and the molten polymer is compressed in the antechamber. By means of this test, the model ((21) with (17) and $q_{no} = 0$) can be validated without the influence of the mold characteristics. The simulated chamber pressure p_{ci} is compared with measurements by means of a pressure-displacement diagram in Figure 9. The results for polypropylene (PP) and two different injection strokes, i. e., different volumes of the melt cushion, are shown. The left curve corresponds to a very small volume while the right curve gives results for a very large volume. It can be inferred from Figure 9 that the model accurately reflects the system's behavior over the whole pressure range, which proves the feasibility of the proposed model.

In the last test scenarios, injection experiments into the two different molds A and B with the filling resistance according to Figure 6 are performed. The first experiment depicted in Figure 10 shows the results for an injection into mold A with rather slow injection speed (approximately 20% of maximum speed). As expected, a very good agreement between the measured and simulated velocity of the screw v_s can be observed. There are slightly larger differences in the cylinder pressure p_{ci}, where the largest difference occurs at the beginning of the injection process. In this phase of the injection process, the screw touches the melt cushion after moving over the decompression stroke and the non-return valve mounted on the screw closes. Since the closing of the non-return valve is modeled in an idealized way in this paper, the model shows a sharper transition of the cylinder pressure p_{ci} in the simulation compared to

Post-print version of the article: C. Fröhlich, W. Kemmetmüller, and A. Kugi, "Control-oriented modeling of servo-pump driven injection molding machines in the filling and packing phase", *Mathematical and Computer Modelling of Dynamical Systems*, vol. 24, pp. 451–474, 2018. DOI: 10.1080/13873954.2018.1481870

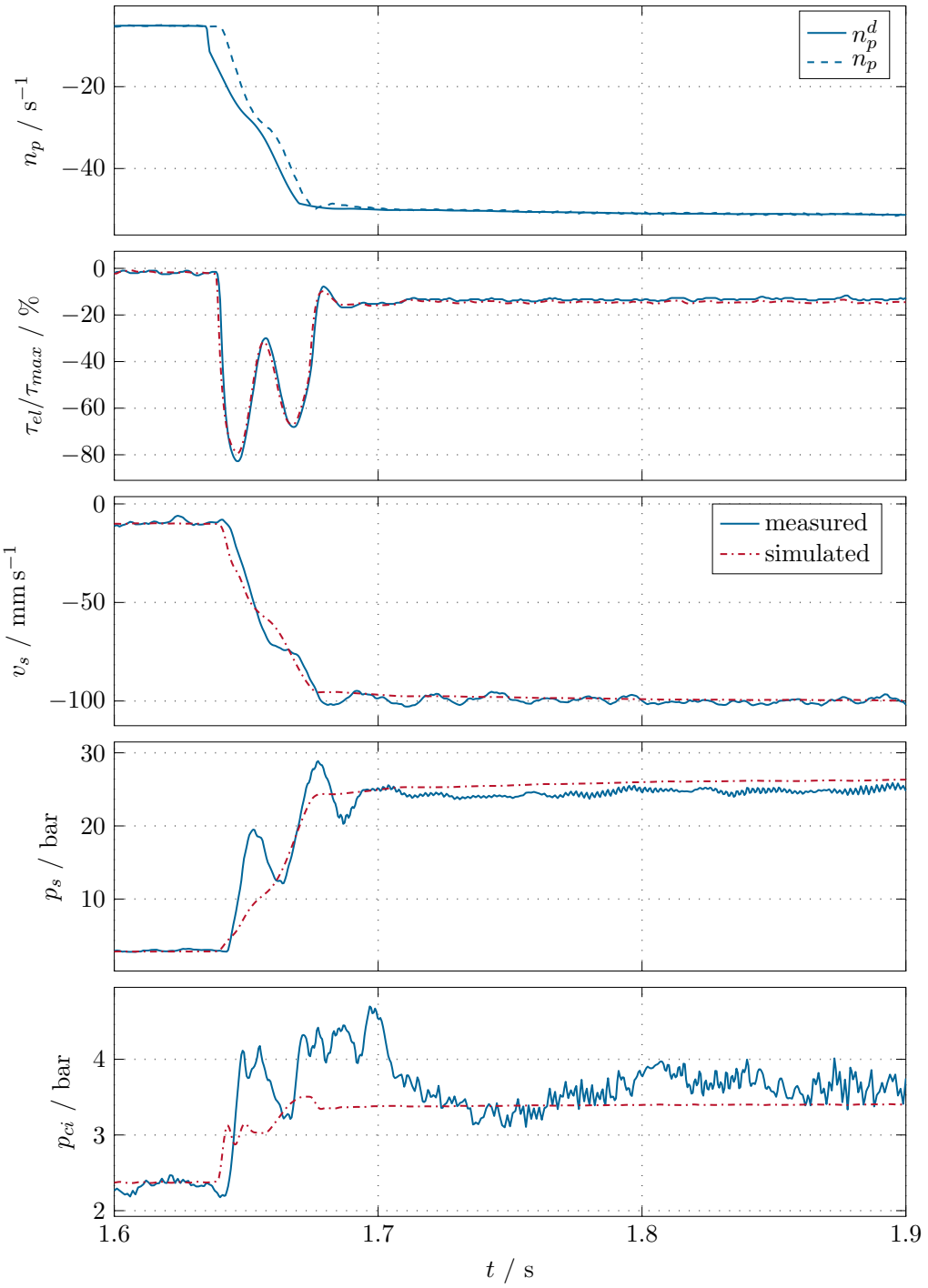

Figure 8.: Validation of the mathematical model for a dry run, picture detail of Figure 7.

Post-print version of the article: C. Fröhlich, W. Kemmetmüller, and A. Kugi, "Control-oriented modeling of servo-pump driven injection molding machines in the filling and packing phase", *Mathematical and Computer Modelling of Dynamical Systems*, vol. 24, pp. 451–474, 2018. DOI: 10.1080/13873954.2018.1481870
The content of this post-print version is identical to the published paper but without the publisher's final layout or copy editing.

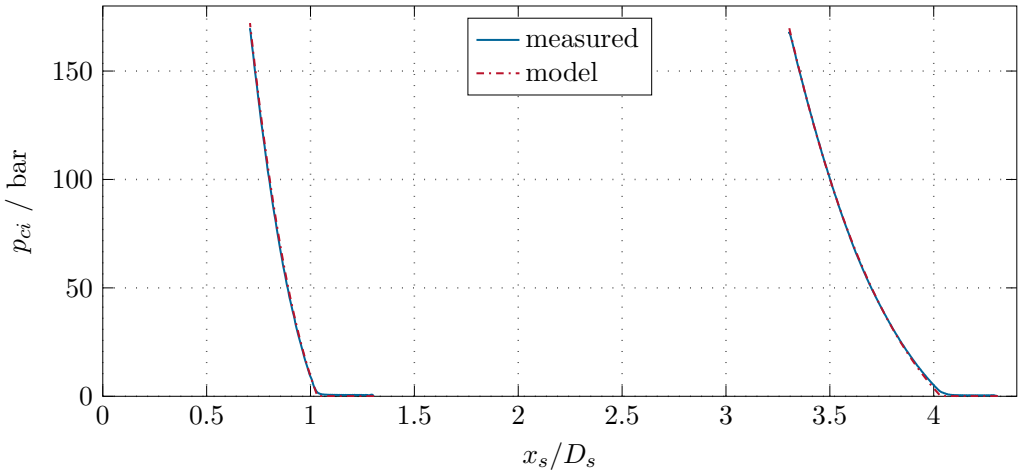

Figure 9.: Pressure-displacement diagram for polypropylene with a small volume of the melt cushion on the left and a large volume on the right.

the measurement. This part of the injection phase is not of great importance for the final product quality, which is why this deviation does not play an important role, in particular for the controller design.

In the next step, a different velocity trajectory with different injection speed is investigated. Figure 11 depicts an experiment with mold A for a significantly increased velocity (almost maximum speed). Clearly, the simulation model is also capable of accurately describing this scenario and thus proves the validity of the model in the whole operating range of the IMM.

Finally, the scalability of the proposed model to different mold geometries is analyzed in the measurements depicted in Figure 12. As discussed in Section 3.3.2, mold B has a different length and width, and thus a different filling behavior. The results of Figure 12 confirm that the model is also perfectly suitable for simulating different mold geometries.

Post-print version of the article: C. Fröhlich, W. Kemmetmüller, and A. Kugi, "Control-oriented modeling of servo-pump driven injection molding machines in the filling and packing phase", *Mathematical and Computer Modelling of Dynamical Systems*, vol. 24, pp. 451–474, 2018. DOI: 10.1080/13873954.2018.1481870

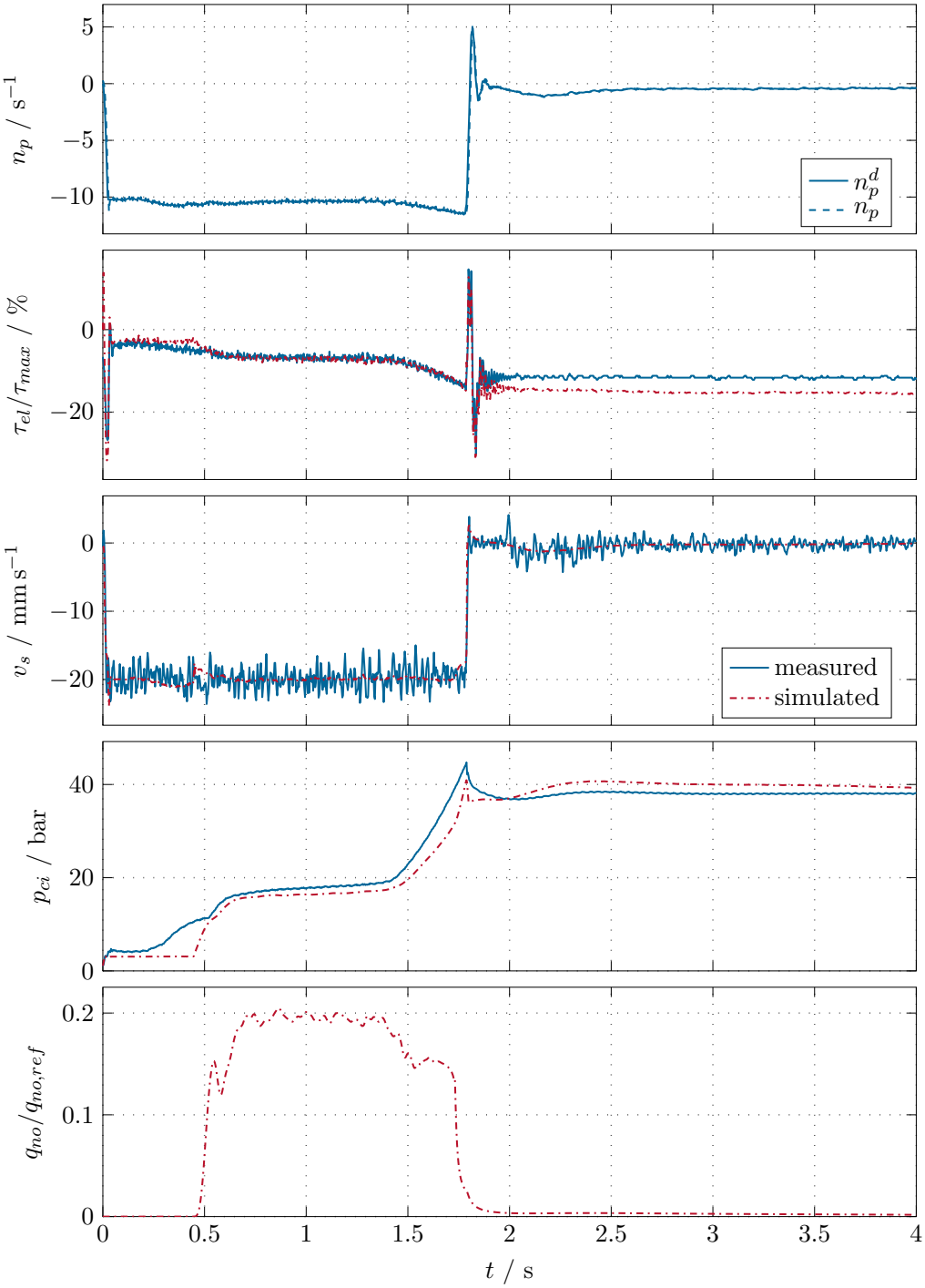

Figure 10.: Injection into mold A with slow injection speed.

Post-print version of the article: C. Fröhlich, W. Kemmetmüller, and A. Kugi, "Control-oriented modeling of servo-pump driven injection molding machines in the filling and packing phase", *Mathematical and Computer Modelling of Dynamical Systems*, vol. 24, pp. 451–474, 2018. DOI: 10.1080/13873954.2018.1481870

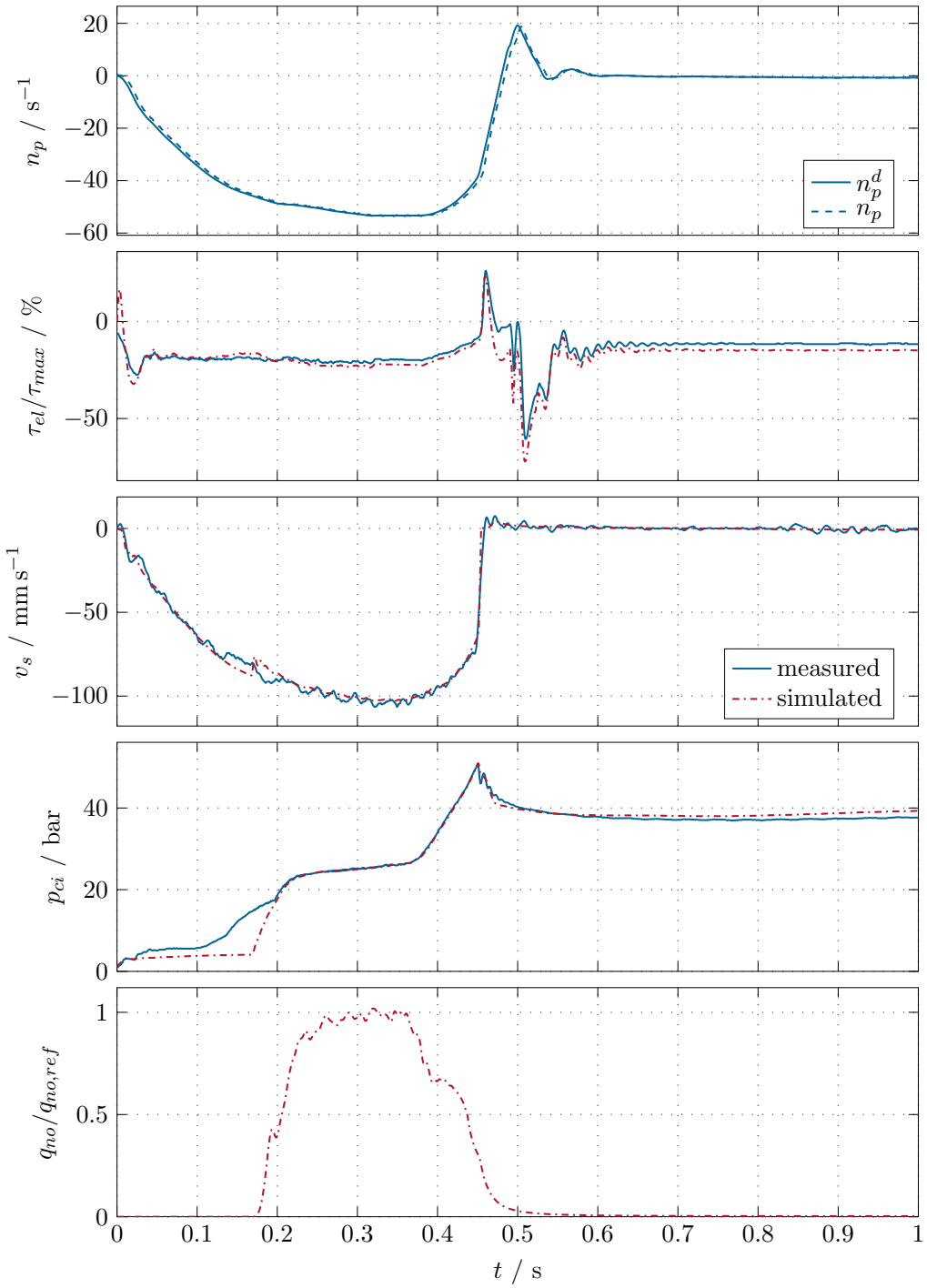

Figure 11.: Injection into mold A with high injection speed.

Post-print version of the article: C. Fröhlich, W. Kemmetmüller, and A. Kugi, "Control-oriented modeling of servo-pump driven injection molding machines in the filling and packing phase", *Mathematical and Computer Modelling of Dynamical Systems*, vol. 24, pp. 451–474, 2018. DOI: 10.1080/13873954.2018.1481870

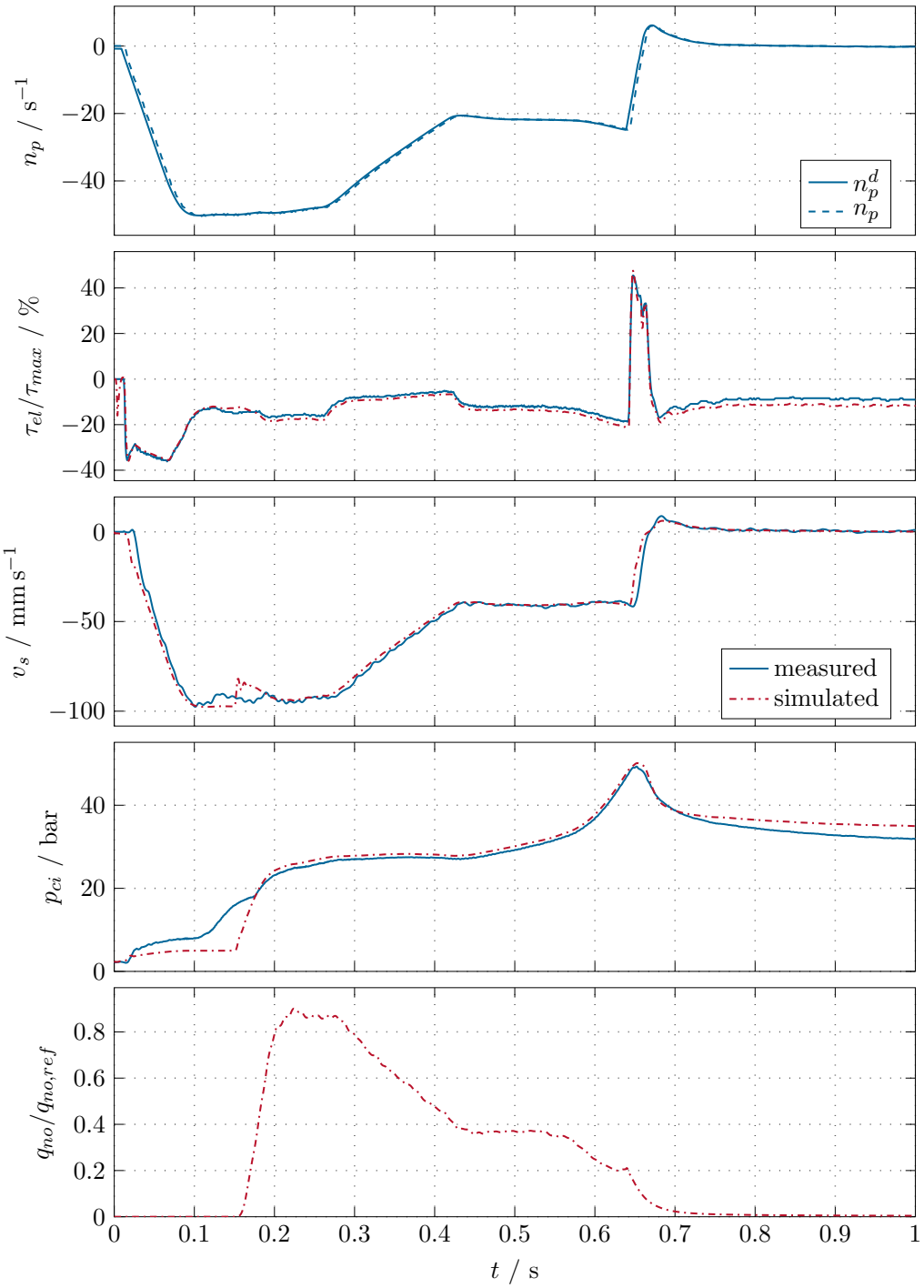

Figure 12.: Injection into mold B.

Post-print version of the article: C. Fröhlich, W. Kemmetmüller, and A. Kugi, "Control-oriented modeling of servo-pump driven injection molding machines in the filling and packing phase", *Mathematical and Computer Modelling of Dynamical Systems*, vol. 24, pp. 451–474, 2018. DOI: 10.1080/13873954.2018.1481870

5. Conclusions

In the present work, a computationally efficient and scalable mathematical model of a hydraulic injection molding unit with a servo-pump is proposed. It combines a first-principles model of the hydraulic actuator system with a phenomenological process model of the injection process. The model accuracy was thoroughly validated by comparing simulation with measurement results. The model features a low computational complexity and can be easily parametrized by geometry parameters of the specific injection molding machine, nominal parameters of the oil, tabulated material parameters of the polymer used, and some friction and process model parameters must be identified based on measurements.

This model serves as an ideal basis for real-time applications and the design of model-based control strategies. Current work deals with the development of a model-predictive control strategy for the injection molding machine, where first experimental results show a significant improvement in comparison to results known from existing controllers.

Nomenclature

Table 1.: Description of symbols and their corresponding units.

Symbol	Definition	Unit
A_{ac}	cross-sectional area of the screw	m^2
A_{ci}	cross-sectional area of the hydraulic cylinder	m^2
A_{no}	cross-sectional area of the nozzle	m^2
A_{sv}	opening area of the valve	m^2
$b_i, i = 1, \ldots, 9$	parameters for the Tait equation	mixed
D_s	screw diameter	m
d_c	Coulomb friction coefficient	N
$d_{c,mot}$	Coulomb friction coefficient	$\mathrm{N\,m}$
d_q	quadratic friction coefficient	$\mathrm{N\,s^2\,m^{-2}}$
d_s	friction parameter for $F_{fr,s}$	$\mathrm{N\,s^n\,m^{-n}}$
d_v	viscous friction coefficient	$\mathrm{N\,s\,m^{-1}}$
$d_{v,mot}$	viscous friction coefficient	$\mathrm{N\,m\,s}$
F_{fr}	overall friction force	N
$F_{fr,c}$	friction force in the cylinder	N
$F_{fr,s}$	friction force between the screw and the barrel	N
F_{tot}	overall force acting on the hydraulic pistons	N
J_p	inertia of the pump	$\mathrm{N\,m\,s^{-1}}$
l_0	length of the wetted cylinder surface	m
$\dot{m}_p$	mass flow generated by the pump	$\mathrm{kg\,s^{-1}}$
m_s	overall mass	kg
$\dot{m}_{sv}$	mass flow of the servo-valve	$\mathrm{kg\,s^{-1}}$
n	flow behavior index	–
n_p	pump speed	$\mathrm{s^{-1}}$
n_p^d	desired pump speed	$\mathrm{s^{-1}}$
p_0	ambient pressure	Pa
p_{ac}	pressure in the antechamber	Pa

Continued on next page

Post-print version of the article: C. Fröhlich, W. Kemmetmüller, and A. Kugi, "Control-oriented modeling of servo-pump driven injection molding machines in the filling and packing phase", *Mathematical and Computer Modelling of Dynamical Systems*, vol. 24, pp. 451–474, 2018. DOI: 10.1080/13873954.2018.1481870

Table 1 – continued from previous page

Symbol	Definition	Unit
p_{ci}	pressure in the injection chambers	Pa
p_t	tank pressure	Pa
$p_{vap,l}$	lower vapor pressure	Pa
$p_{vap,u}$	upper vapor pressure	Pa
p_{voln}	pressure for volumetric efficiency η_{voln}	Pa
p_p	pump pressure	Pa
q_{no}	volume flow into the mold	$\mathrm{m^3\,s^{-1}}$
r_{fz}	resistance parameter for $r_{no,t}$	$\mathrm{Pa\,s^n\,m^{-n}}$
$r_{no,t}$	time-dependent filling resistance	$\mathrm{Pa\,s^n\,m^{-n}}$
$r_{no,x}$	position-dependent filling resistance	$\mathrm{Pa\,s^n\,m^{-n}}$
r_{no}	filling resistance	$\mathrm{Pa\,s^n\,m^{-n}}$
r_s	stiffness of screw	$\mathrm{m\,Pa^{-1}}$
T_{ac}	polymer temperature	K
t_{dt}	dead-time	s
t_{fe}	time when $x_{s,fe}$ is reached	s
t_{fz1}, t_{fz2}	time constants for $r_{no,t}$	s
V_{ac}	volume of the antechamber	$\mathrm{m^3}$
V_{ci0}	volume of one injection chamber for $x_s = 0$	$\mathrm{m^3}$
V_{th}	geometrical displacement volume	$\mathrm{m^3}$
V_p	volume of the supply line	$\mathrm{m^3}$
v_{ac}	specific volume of the polymer in the antechamber	$\mathrm{m^3\,kg^{-1}}$
v_{t0}	reference velocity for Coulomb friction	$\mathrm{m\,s^{-1}}$
v_s	screw velocity	$\mathrm{m\,s^{-1}}$
$x_{s,f0}$	screw position at the beginning of the filling phase	m
$x_{s,fe}$	screw position at the end of the filling phase	m
x_s	screw position	m
x_s^{stop}	mechanical end stop	m
α_{sv}	contraction coefficient	–
β	bulk modulus	Pa
$\beta_i, i = 0, 1, 2$	parameters for bulk modulus β_{ac}	mixed
$\Delta x_{s,mo}$	displacement of the screw required to fill the mold	m
η_{hm}	hydromechanic efficiency	–
η_{vol}	volumetric efficiency	–
η_{vol0}	volumetric efficiency at p_0	–
η_{voln}	volumetric efficiency at p_{voln}	–
ϱ	mass density	$\mathrm{kg\,m^{-3}}$
τ_{el}	torque of electric drive	N m
τ_{fr}	friction torque	N m
$\tau_{p,hm}$	hydromechanic pump torque	N m
τ_p	theoretical pump torque	N m

References

[1] T.A. Osswald, L.S. Turng, and P. Gramann, „Injection Molding Handbook“, Carl Hanser Verlag, Munich, Germany, 2008.

Post-print version of the article: C. Fröhlich, W. Kemmetmüller, and A. Kugi, “Control-oriented modeling of servo-pump driven injection molding machines in the filling and packing phase”, *Mathematical and Computer Modelling of Dynamical Systems*, vol. 24, pp. 451–474, 2018. DOI: 10.1080/13873954.2018.1481870
The content of this post-print version is identical to the published paper but without the publisher’s final layout or copy editing.

[2] R.S. Spencer and G.D. Gilmore, „Some flow phenomena in the injection molding of polystyrene“, Journal of Colloid Science 6 (1951), pp. 118–132.
[3] R.E. Nunn and R.T. Fenner, „Flow and heat transfer in the nozzle of an injection molding machine“, Polymer Engineering and Science 77 (1977).
[4] D.G.F. Huilier, „Modeling of injection mold post-filling: A review and some critical problems to solve“, Journal of Polymer Engineering 9 (1990), pp. 237–302.
[5] R. Zheng, X.J. Fan, and R.I. Tanner, „Injection Molding: Integration of Theory and Modeling Methods“, Springer, Berlin, Germany, 2011.
[6] P. Kennedy and R. Zheng, „Flow Analysis of Injection Molds“, Carl Hanser Verlag, Munich, Germany, 2013.
[7] D. Abu Fara, „The dynamics of injection hydraulics in thermoplastics injection molding“, Ph.D. diss., McGill University, Montreal, Canada, 1983.
[8] K.K. Wang, „Injection molding modelling, progress report“, Cornell University (1984).
[9] I.O. Pandelidis and A.R. Agrawal, „Optimal anticipatory control of ram velocity in injection molding“, Polymer Engineering and Science 28 (1988), pp. 147–156.
[10] H.P. Tsoi and F. Gao, „Control of injection velocity using a fuzzy logic rule-based controller for thermoplastics injection molding“, Polymer Engineering and Science 39 (1999), pp. 3–17.
[11] M.R. Kamal, W.I. Patterson, N. Conley, D. Abu Fara, and G. Lohfink, „Dynamics and control of pressure in the injection molding of thermoplastics“, Polymer Engineering and Science 27 (1987), pp. 1403–1410.
[12] C.P. Chiu, J.H. Wei, and M.C. Shih, „Adaptive model following control of the mold filling process in an injection molding machine“, Polymer Engineering and Science 31 (1991), pp. 1123–1129.
[13] S.M. Smud, D.O. Harper, P.B. Deshpande, and K.W. Leffew, „Advanced process control for injection molding“, Polymer Engineering and Science 31 (1991), pp. 1081–1085.
[14] M. Abu-Ayyad and R. Dubay, „Development of an extended predictive controller for injection speed“, in „Proc. of ANTEC 2007, Ohio, USA“, Vol. 2. 2007, pp. 680–683.
[15] M. Abu-Ayyad, R. Dubay, and J.M. Hernandez, „A nonlinear model-based predicitve controller for injection speed“, in „Proc. of ANTEC 2009, Illinois, USA“, Vol. 5. 2009, pp. 2923–2929.
[16] M.R. Kamal, W.I. Patterson, D.A. Fara, and A. Haber, „A study in injection molding dynamics“, Polymer Engineering and Science 24 (1984), pp. 686–691.
[17] F. Gao, W.I. Patterson, and M.R. Kamal, „Self-tuning cavity pressure control of injection molding filling“, Advances in Polymer Technology 13 (1994), pp. 111–120.
[18] A.E. Varela, „Self-tuning pressure control in an injection moulding cavity during filling“, Chemical Engineering Research and Design 78 (2000), pp. 79–86.
[19] J. Shi, F. Gao, and T.J. Wu, „From two-dimensional linear quadratic optimal control to iterative learning control. Paper 1. Two-dimensional linear quadratic optimal controls and system analysis“, Industrial & Engineering Chemistry Research 45 (2006), pp. 4603–4616.
[20] R. Dubay, B. Pramujati, J. Han, and F. Strohmaier, „An investigation on the application of predictive control for controlling screw position and velocity on an injection molding machine“, Polymer Engineering and Science 47 (2007), pp. 390–399.
[21] M.A.C. Finn, J.M. Hernández, and R. Dubay, „Cavity peak pressure control during packing using model precictive control theory“, in „Proc. of ANTEC 2011, Newton, USA“. 2011, pp. 2408–2412.
[22] C. Hopmann, D. Abel, J. Heinisch, and S. Stemmler, „Self-optimizing injection molding based on iterative learning cavity pressure control“, Production Engineering 11 (2017), pp. 97–106.
[23] F. Gao, Y. Yang, and C. Shao, „Robust iterative learning control with applications to injection molding process“, Chemical Engineering Science 56 (2001), pp. 7025–7034.
[24] R. Lakhram and R. Dubay, „Self-Optimizing MPC of Injection Velocity During Mold Fill“, in „Proc. of ANTEC 2002, San Francisco, USA“, Vol. 3. 2002.
[25] C.M. Dong and A.A. Tseng, „A multivariable self-tuning controller for injection molding

Post-print version of the article: C. Fröhlich, W. Kemmetmüller, and A. Kugi, “Control-oriented modeling of servo-pump driven injection molding machines in the filling and packing phase”, *Mathematical and Computer Modelling of Dynamical Systems*, vol. 24, pp. 451–474, 2018. DOI: 10.1080/13873954.2018.1481870
The content of this post-print version is identical to the published paper but without the publisher’s final layout or copy editing.

machines“, Computers in Industry 13 (1989), pp. 107–122.
[26] Y. Yang and F. Gao, „Adaptive control of the filling velocity of thermoplastics injection molding“, Control Engineering Practice 8 (2000), pp. 1285–1296.
[27] Y. Yang, K. Yao, and F. Gao, „Overall control system for injection molding process“, International Polymer Processing 27 (2012), pp. 40–59.
[28] R. Dubay, „Predictive control of cavity pressure during injection filling“, Journal of Injection Molding Technology 5 (2001), pp. 72–79.
[29] B. Pramujati, R. Dubay, and J.G. Han, „Injection velocity control in plastic injection molding“, in „Proc. of ANTEC 2005, Boston, USA“, Vol. 2. 2005, pp. 305–309.
[30] T. Petrova and D. Kazmer, „Hybrid neural models for pressure control in injection molding“, Advances in Polymer Technology 18 (1999), pp. 19–31.
[31] W. Michaeli and A. Schreiber, „Online control of the injection molding process based on process variables“, Advances in Polymer Technology 28 (2009), pp. 65–76.
[32] S. Kenig, A. Ben-David, M. Omer, and A. Sadeh, „Control of properties in injection molding by neural networks“, Engineering Applications of Artificial Intelligence 14 (2001), pp. 819–823.
[33] A. Shankar and F.W. Paul, „A mathematical model for the evaluation of injection molding machine control“, Journal of Dynamic Systems, Measurement, and Control 104 (1982), pp. 86–92.
[34] J. Hu and J.H. Vogel, „Dynamic modeling and control of packing pressure in injection“, Journal of Engineering Materials and Technology 116 (1994), pp. 244–249.
[35] D. Kazmer and P. Barkan, „The process capability of multi-cavity pressure control for the injection molding process“, Polymer Engineering and Science 37 (1997), pp. 1880–1895.
[36] I. Yigit, Y. Ercan, and S. Saritas, „Cavity pressure control of powder injection moulding machines“, Transactions of the Institute of Measurement and Control 26 (2004), pp. 393–415.
[37] M. Rafizadeh, W.I. Patterson, and M.R. Kamal, „Physically-based model of thermoplastics injection molding for control applications“, International Polymer Processing 11 (1996), pp. 352–362.
[38] M. Rafizadeh, W.I. Patterson, and M.R. Kamal, „Physically-based adaptive control of cavity pressure in injection moulding process: Packing phase“, Iranian Polymer Journal (English Edition) 8 (1999), pp. 99–113.
[39] C.P. Chiu, L.C. Shih, and J.H. Wei, „Dynamic modeling of the mold filling process in an injection molding machine“, Polymer Engineering and Science 31 (1991), pp. 1417–1425.
[40] S.L.B. Woll and D.J. Cooper, „A dynamic injection-molding process model for simulating mold cavity pressure patterns“, Polymer-Plastics Technology and Engineering 36 (1997), pp. 809–840.
[41] Y.J. Cho, H.S. Cho, and C.O. Lee, „Optimal open-loop control of the mould filling process for injection moulding“, Optimal Control Applications and Methods 4 (1983), pp. 1–12.
[42] Y.W. Lin and J.W.J. Cheng, „Model-based melt flow virtual sensors for filling process of injection molding“, Polymer Engineering and Science 48 (2008), pp. 543–555.
[43] H. Daxberger, K. Rieger, and K. Schlacher, „On modelling and control of compressible non-Newtonian injection processes“, in „Computer Aided Systems Theory – EUROCAST 2011“, Lecture Notes in Computer Science Vol. 6928, Springer, Berlin, Germany, 2012, pp. 65–72.
[44] D. Dorner, T. Radermacher, B. Wagner, and J. Weber, „Iterative learning control of a plastics injection molding machine (in German), Iterativ Lernende Regelung einer Kunststoff-Spritzgießmaschine“, at - Automatisierungstechnik 62 (2014), pp. 226–236.
[45] D. Zheng and A. Alleyne, „Modeling and control of an electro-hydraulic injection molding machine with smoothed fill-to-pack transition“, Journal of Manufacturing Science and Engineering 125 (2003), pp. 154–163.
[46] M. Reiter, S. Stemmler, C. Hopmann, A. Reßmann, and D. Abel, „Model Predictive Control of Cavity Pressure in an Injection Moulding Process“, in „Proc. of the 19th IFAC World Congress“, Vol. 47, Cape Town, South Africa. 2014, pp. 4358–4363.

Post-print version of the article: C. Fröhlich, W. Kemmetmüller, and A. Kugi, “Control-oriented modeling of servo-pump driven injection molding machines in the filling and packing phase”, *Mathematical and Computer Modelling of Dynamical Systems*, vol. 24, pp. 451–474, 2018. DOI: 10.1080/13873954.2018.1481870
The content of this post-print version is identical to the published paper but without the publisher’s final layout or copy editing.

[47] K.K. Tan, S.N. Huang, and X. Jiang, „Adaptive control of ram velocity for the injection moulding machine“, IEEE Transactions on Control Systems Technology 9 (2001), pp. 663–671.
[48] S.O. Lindert, G. Reindl, and K. Schlacher, „Identification and Control of an Injection Moulding Machine“, in „Proc. of the 19th IFAC World Congress“, Vol. 47, Cape Town, South Africa. 2014, pp. 5878–5883.
[49] M. Rafizadeh, W.I. Patterson, and M.R. Kamal, „Physically-based adaptive control of cavity pressure in injection molding: Filling phase“, International Polymer Processing 12 (1997), pp. 385–394.
[50] H. Havlicsek and A. Alleyne, „Nonlinear modeling of an electrohydraulic injection molding machine“, in „Proc. of the American Control Conference 1999, San Diego, USA“, Vol. 1. 1999, pp. 171–175.
[51] X. He, X. Wang, Z. Feng, and Z. Zhang, „Nonlinear modeling of electrohydraulic servo injection molding machine including asymmetric cylinder“, in „Proc. of the American Control Conference 2003, Denver, USA“, Vol. 4. 2003, pp. 3055–3059.
[52] J.H. Wei, C.C. Chang, and C.P. Chiu, „A nonlinear dynamic model of a servo-pump controlled injection molding machine“, Polymer Engineering and Science 34 (1994), pp. 881–887.
[53] S. Wang, J. Ying, Z. Chen, and K. Cai, „Grey fuzzy PI control for packing pressure during injection molding process“, Journal of Mechanical Science and Technology 25 (2011), pp. 1061–1068.
[54] Y.g. Peng, J. Wang, and W. Wei, „Model predictive control of servo motor driven constant pump hydraulic system in injection molding process based on neurodynamic optimization“, Journal of Zhejiang University Science C 15 (2014), pp. 139–146.
[55] J.P. Franc and J.M. Michel, „Fundamentals of Cavitation“, Fluid Mechanics and Its Applications Vol. 76, Kluwer Academic Publishers, Dordrecht, Netherlands, 2005.
[56] K. Prinz, W. Kemmetmüller, and A. Kugi, „Mathematical modelling of a diesel common-rail system“, Mathematical and Computer Modelling of Dynamical Systems 21 (2014), pp. 311–335.
[57] P. Casoli, A. Vacca, G. Franzoni, and G.L. Berta, „Modelling of fluid properties in hydraulic positive displacement machines“, Simulation Modelling Practice and Theory 14 (2006), pp. 1059–1072.
[58] D.W. van Krevelen and K. te Nijenhuis, „Properties of Polymers“, 4th ed., Elsevier, Oxford, United Kingdom, 1990.
[59] D. Kazmer, „Injection Mold Design Engineering“, Carl Hanser Verlag, Munich, Germany, 2007.

Post-print version of the article: C. Fröhlich, W. Kemmetmüller, and A. Kugi, “Control-oriented modeling of servo-pump driven injection molding machines in the filling and packing phase”, *Mathematical and Computer Modelling of Dynamical Systems*, vol. 24, pp. 451–474, 2018. DOI: 10.1080/13873954.2018.1481870
The content of this post-print version is identical to the published paper but without the publisher’s final layout or copy editing.